*Express Polymer Letters Vol.18, No.9 (2024) 942–949*
*Available online at www.expresspolymlett.com*
*https://doi.org/10.3144/expresspolymlett.2024.71*

*Letter article*

# Controllable design and modeling of gradient porous structures by phase field theory

*Hangming Shen*[1], *Xingzhe Zhao*[1], *Lihong Yang*[1*], *Jiantao Yang*[2]

[1]School of Mechanical Engineering, University of Shanghai for Science and Technology, 200093 Shanghai, China
[2]Institute of Rehabilitation Engineering and Technology, University of Shanghai for Science and Technology, 200093 Shanghai, China

*Received 5 May 2024; accepted in revised form 25 June 2024*

**Abstract.** In this study, a novel methodology for the fabrication of gradient porous structures is introduced, predicated upon the phase evolution characteristics of immiscible polymer blends. Initially, a comprehensive flow-phase field dynamics model is developed. This model couples the principles of phase field theory and the dynamics of fluid flow to the two-phase evolution process, facilitating a numerical simulation of the phase evolution. Subsequently, the phase field parameters of model are determined and combined with the temperature field, thereby enabling a targeted and controlled fabrication of gradient porous structures. Finally, the efficacy and practical applicability of the proposed methodology are substantiated through the construction of illustrative examples. This approach, as delineated herein, provides a robust framework for the efficient design and realization of intricate, interconnected gradient porous structures with potential applications in various scientific and engineering domains.

***Keywords:*** *functional structure, porosity, gradient porous structure, phase field, temperature field*

## 1. Introduction

Gradient porous structures, characterized by spatial variation in porosity or pore size that changes gradually in one or more directions, exhibit superior performance and have found applications across various fields. Traditional methods for creating such structures often struggle with precise control over pore size, porosity, and their spatial distribution. However, the advancement of additive manufacturing technology opens new avenues for fabricating gradient porous structures, contingent upon sound and efficient geometric modeling [1, 2]. An adept modeling approach not only significantly reduces the design and manufacturing timeline but also ensures product quality, playing a pivotal role in the structural design process.

Computer aided design (CAD) modeling is the predominant approach for designing gradient porous structures. It starts with designing simple pore elements and then assembles these into gradient porous structures through Boolean operations. While straightforward and convenient, this method best suits the modeling of structures with regularly and orderly arranged pores [3]. However, the demand in practical applications often leans towards gradient porous structures featuring irregular and interconnected pores. These structures are crucial in various applications, including bone tissue engineering scaffolds in biomedical engineering [4, 5], filtration and separation technology for water treatment and air purification [6, 7], energy storage and conversion in batteries [8, 9], heat dissipation of electronic equipment [10], and noise from acoustic materials control [11], *etc*. The challenge in modeling these applications lies in constructing irregular and interconnected pores and controlling complex pore size distributions.

*Corresponding author, e-mail: lhyang@usst.edu.cn

Consequently, parametric modeling of gradient porous structures, utilizing a series of algorithms, has emerged as a focal point of research.

Algorithm-based approaches to designing gradient porous structures mainly encompass the Voronoi tessellation method and the implicit surface method. The Voronoi method creates a grid structure by generating a series of random discrete points and then logically connecting these points using various design strategies [4, 12]. However, this method faces challenges such as lack of repeatability, high energy consumption, and extended processing time. On the other hand, the implicit surface method, exemplified by Three Periodic Minimal Surfaces (TPMS) that are periodic in three mutually independent directions in three-dimensional space, allows for the manipulation of structural properties by altering parameters in the mathematical equation [13, 14]. While this method is user-friendly, achieving complex pore size distributions remains a challenge.

In our previous research, co-continuous gradient porous structures were fabricated from immiscible polymer blends via "temperature difference phase separation" [15, 16]. This approach was centered on the phase evolution process of such blends, utilizing their natural immiscibility and the temperature-dependency of their phase evolution rates. The application of a temperature field enabled the precise control of porosity gradient distributions, ultimately the interconnected gradient porous structures with different pore size distributions. Motivated by these insights, in this work, a model coupling phase field theory with fluid flow dynamics is established, and the phase evolution process of polymer blends is simulated. On this basis, a design method for gradient porous structures based on phase field theory by applying temperature fields is proposed, which provides model data for additive manufacturing technology. The research in this article can enrich the design methods of gradient porous structures.

## 2. Mathematical model

To accurately simulate the phase evolution process of co-continuous polymer blends, the two-phase region is modeled as the fluid domain, with the boundary between these phases treated as the kinematic boundary. This approach allows the preparation process to be conceptualized as a two-phase momentum transfer issue featuring a moving boundary. By integrating phase field theory with fluid dynamics at this interface, a coupled flow-phase field model is established to address the dynamics of a moving two-phase boundary. The behavior of the phase field variable is governed by the Cahn-Hilliard equation [17], as indicated in Equation (1):

$$\frac{\partial \phi}{\partial t} + \mathbf{v} \cdot \nabla \phi = \nabla \cdot \left( M \nabla \frac{\delta F}{\delta \phi} \right) \tag{1}$$

where, $\phi$ is the phase field variable, $t$ is the time, $\mathbf{v}$ is the velocity vector, $M$ is the mobility coefficient. $F$ is the total free energy of the mixed system, which can be expressed as Equation (2):

$$F = \int_V \left[ f_0 + \frac{\kappa}{2} (\nabla \phi)^2 \right] \mathrm{d}V \tag{2}$$

$\kappa$ is the gradient energy coefficient, and $V$ is the volume of the object.

The Ginzburg-Landau free energy functional, better suited for binary immiscible systems, is substituted into Equation (1), from which the phase field equation is derived, as demonstrated in Equation (3):

$$\frac{\partial \phi}{\partial t} + \mathbf{v} \cdot \nabla \phi = \nabla \cdot \left( \frac{M\kappa}{\varepsilon^2} \nabla \left[ \phi \left( \phi^2 - 1 \right) + \nabla \cdot \left( \varepsilon^2 \nabla \phi \right) \right] \right) \tag{3}$$

where, $\varepsilon$ is the interface thickness.

As $\varepsilon$ tends to 0, the ratio $\frac{\kappa}{\varepsilon}$ produces interfacial tension (Equation (4)):

$$\sigma = \frac{2\sqrt{2}}{3} \frac{\kappa}{\varepsilon} \tag{4}$$

in the classical sense [18], and the mobility adjustment parameter is defined as(Equation (5)):

$$\chi = \frac{M}{\varepsilon^2} \tag{5}$$

Using parameters $\sigma$ and $\chi$, Equation (2) can be expressed in another form (Equation (6)):

$$\frac{\partial \phi}{\partial t} + \mathbf{v} \cdot \nabla \phi = = \nabla \cdot \left( \frac{3\varepsilon \chi \sigma}{2\sqrt{2}} \nabla \left[ \phi \left( \phi^2 - 1 \right) + \nabla \cdot \left( \varepsilon^2 \nabla \phi \right) \right] \right) \tag{6}$$

The fluid flow in a fixed area is governed by the coupling of mass and momentum conservation, which can be expressed by the Equation (7):

$$\begin{cases} \nabla \cdot \mathbf{v} = 0 \\ \nabla \cdot \left[ \eta \left( \nabla \mathbf{v} + (\nabla \mathbf{v})^{\mathrm{T}} \right) \right] = 0 \end{cases} \tag{7}$$

where $T$ is the transposition of the matrix in Equation (7); η is the viscosity.

During the flow-phase field dynamics model evolution of co-continuous polymer blends, the interface between fluid domains serves as the kinematic boundary and is affected by interfacial tension and size-related factors [19]. In such instances, the integration of the flow model with the boundary convection equation leads to the development of a fluid flow model characterized by a moving boundary. The simulation of the preparation process is conducted using the established mathematical model, which encompasses four parameters: viscosity, interfacial tension, mobility, and interfacial thickness, where the viscosity is determined based on its physical significance.

This study employs the physical process of co-continuous polymer blends to perform geometric modeling of gradient porous structures. In the modeling process, the influence of material viscosity can be disregarded, thus, the process is controlled by three key phase field parameters: interfacial tension, mobility, and interface thickness. The production of a homogeneous porous structure results from isothermal heat treatment (absence of temperature field), while the application of non-isothermal heat treatment (incorporation of temperature field) facilitates the creation of a gradient porous structure with a specific pore size distribution, achieved by the strategic design of a suitable temperature field.

## 3. Modeling process and control strategies

Drawing from the mathematical model established in Section 2 for the phase evolution process of immiscible co-continuous polymer blends, a method for geometric modeling of gradient porous structures has been developed in COMSOL. Illustrated in Figure 1, the procedure begins by setting the design objective, which is to achieve a pore size distribution meets the required performance criteria. Following this, modeling is executed, informed by the simulation of the gradient porous structure's preparation process. The steps involved in modeling process include: constructing the external geometric model of the object, generating a two-phase initial structure at random, manipulating the phase field parameters, and generating a gradient phase structure through temperature field design; subsequently, one phase is removed to achieve the gradient porous structure with the targeted pore size distribution. The completed geometric model is then converted into a file that can be used for additive manufacturing technology data exchange to facilitate subsequent applications.

To ensure a distinct two-phase interface throughout the geometric modeling process, the following approach is adopted for setting the phase field parameters: the computational grid is typically configured as a tetrahedral structure, and the size of the grid is dozens of times smaller than the smallest phase geometric size in the model. The interface thickness is

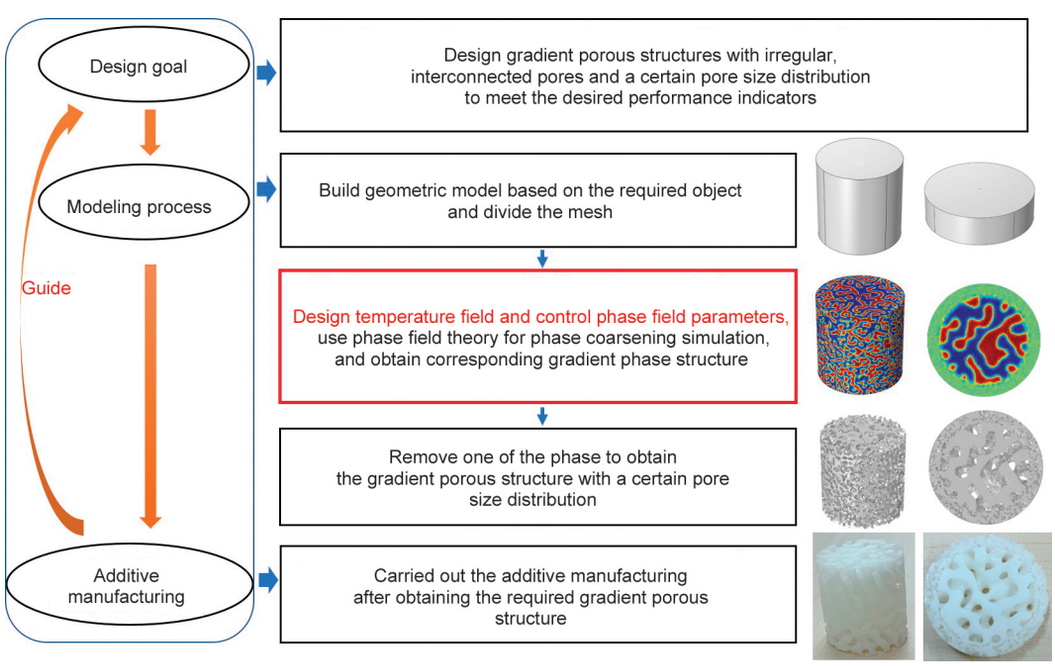


**Figure 1.** Modeling method.

designated as $10^{-3}$ times the average size of the mesh, while the initial mobility parameter is set at 1 m·s/kg. Adjustments to the interfacial tension and time step, followed by the attainment of a stable solution, allow for the recalibration of the mobility value to guarantee accurate tracking of the two-phase interface movement. Once these phase field parameters are established, adjustments to the interfacial tension enable controlled modifications to pore size within specified limits. In the case of a homogeneous porous structure, the pore size is directly influenced by the value of interfacial tension, assuming other conditions are constant. For creating a gradient porous structure, a temperature field is applied. By establishing a relationship between the interfacial tension and the temperature field, the pore size distribution is tuned through the strategic manipulation of the temperature field.

## 4. Results

### 4.1. Modeling of homogeneous porous structure

In this section, a cylinder measuring 30 mm in diameter and 35 mm in height is employed as the outer contour geometric model for simulating homogeneous porous structures with varying pore diameters and porosities. Free tetrahedral meshing is used, with a maximum cell size of 1.11 mm, a minimum cell size of 0.12 mm, and a mesh number of 312742. Based on the mesh size, the interface thickness and mobility are set at 0.045 m and 1 m·s/kg, respectively, while the interfacial tension is varied across four distinct values: 0.1, 0.4, 0.7, and 1 N/m. Following the process outlined in Section 3, one phase is subsequently removed, resulting in the acquisition of homogeneous porous structures featuring four varying pore sizes, all with a porosity of 0.5. These structures are then 3D printed using Stereo Lithography Apparatus (SLA), as depicted in Figure 2a. This figure demonstrates that, under certain conditions, homogeneous porous structures with interconnected different pore diameters can be achieved by varying the interfacial tension values, with the pore diameter increasing as the interfacial tension value rises. Moreover, by maintaining the interfacial tension at a constant value of 0.4 N/m and employing the same modeling procedure, phase components of differing concentrations are eventually removed. This process yields four homogeneous porous structures with varying porosities, as illustrated in Figure 2b.

### 4.2. Modeling of gradient porous structures

Drawing upon the documented applications of gradient porous structures in literature, this section employs the phase field method to design and model such structures. Reference [20] used the TPMS method to simulate a femoral structure with a dense cortical shell and a porous cancellous interior, as depicted in Figure 3a. The pore size transitions from small in the outer region to larger in the central inner region, exhibiting a distinct variation between these sizes. Employing the phase field approach outlined in this paper, a similar structure, mirroring these pore size characteristics, is achieved. The meshing is done using a free tetrahedral mesh. The maximum cell size is 1.01 mm, the minimum cell size is 0.19 mm, and the number of grid cells is 228 492. The interfacial tension σ (in N/m) is set as a piecewise function of the temperature $T$ (in K). The outer temperature is 10 K, and the center temperature is 100 K. When $10 \leq T \leq 15$, $\sigma = 0.0001$; when $15 < T \leq 100$, $\sigma = 0.5$. The interface thickness $\varepsilon_{pf}$ is $0.3 \cdot 10^{-3}$ m, and the mobility $\chi$ is 1 m·s/kg. The model of the structure is displayed in Figure 3b, with its 3D printed counterpart shown in Figure 3c. The outer region with small pore size is in the shape of a ring, with inner and outer radius of 13.5 and 18.0 mm respectively. The equivalent pore size is 0.27 mm in the outer region and 0.90 mm in the inner region.

Figure 4 illustrates how reference [21, 22] utilized the TPMS approach to create various gradient porous structures. Figure 4a presents a hybrid cylinder/half-sphere shaped scaffold, intended to replicate a femoral head joint. The scaffold consists of a hemisphere with a radius of 20 mm and a cylinder with a radius of 10 mm and a height of 20 mm, and the hemisphere is located directly above the cylinder and closely fits the cylinder, and the axes of both of them are completely overlapped. The phase field method outlined in this paper is employed. The maximum cell size is 1.48 mm, the minimum cell size is 0.16 mm, and the number of grid cells is 120 204. The interfacial tension σ (in N/m) is a piecewise function relative to the temperature $T$ (in K). The temperature gradient is along the Z axis, when $-20 \leq T \leq 0$, $\sigma = 0.001$, when $0 < T \leq 20$, $\sigma = 0.3$. The interface thickness $\varepsilon_{pf}$ is $0.5 \cdot 10^{-3}$ m, and the mobility $\chi$ is 1 m·s/kg. The 3D printed counterpart is produced using the SLA technique, as depicted in Figure 4b. The equivalent pore size of the cylinder part is 0.98 mm, and the

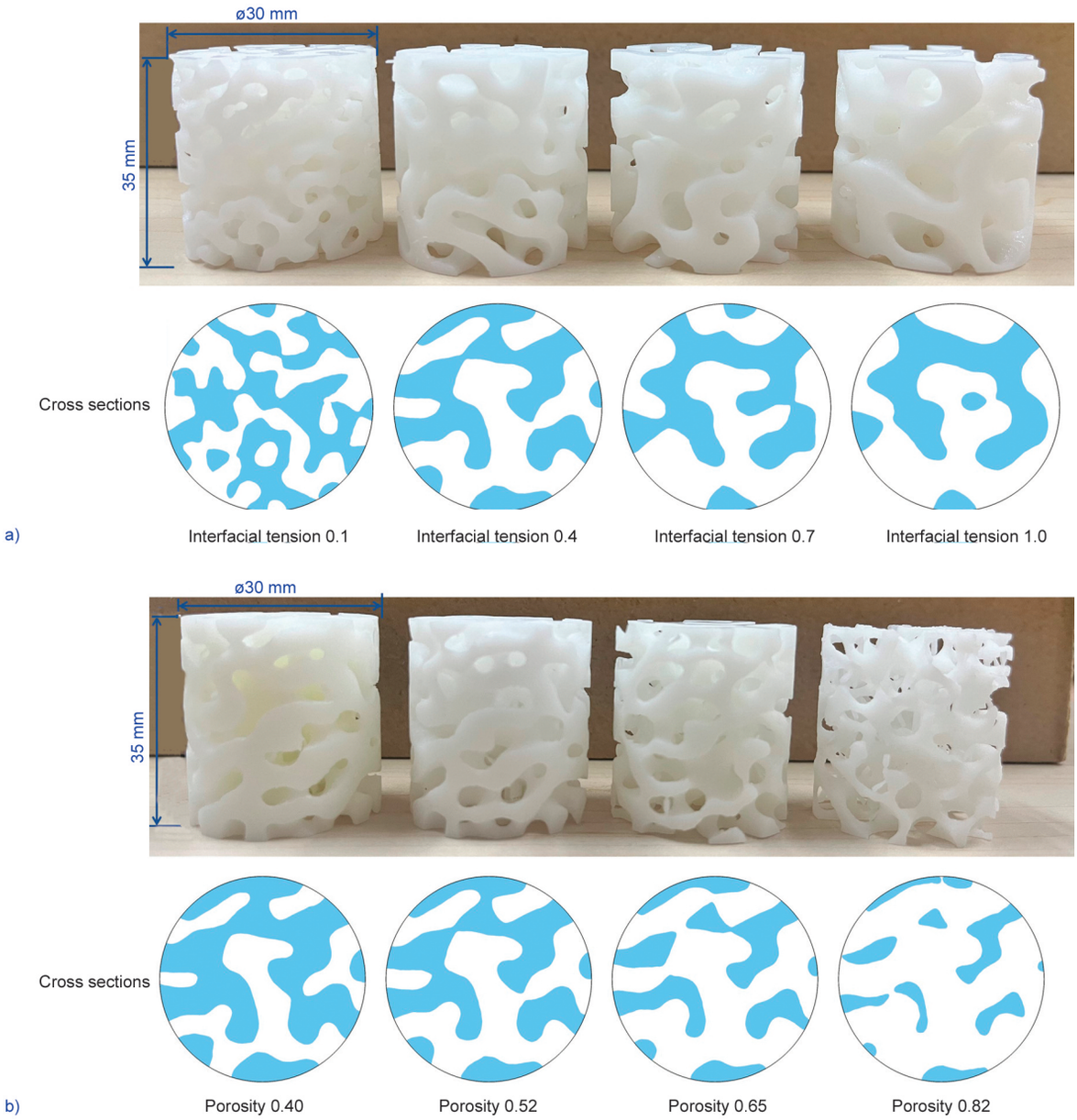


**Figure 2.** Homogeneous porous structures. a) Homogeneous porous structures with different pore sizes (same porosity), b) homogeneous porous structures with different porosities (same pore size).

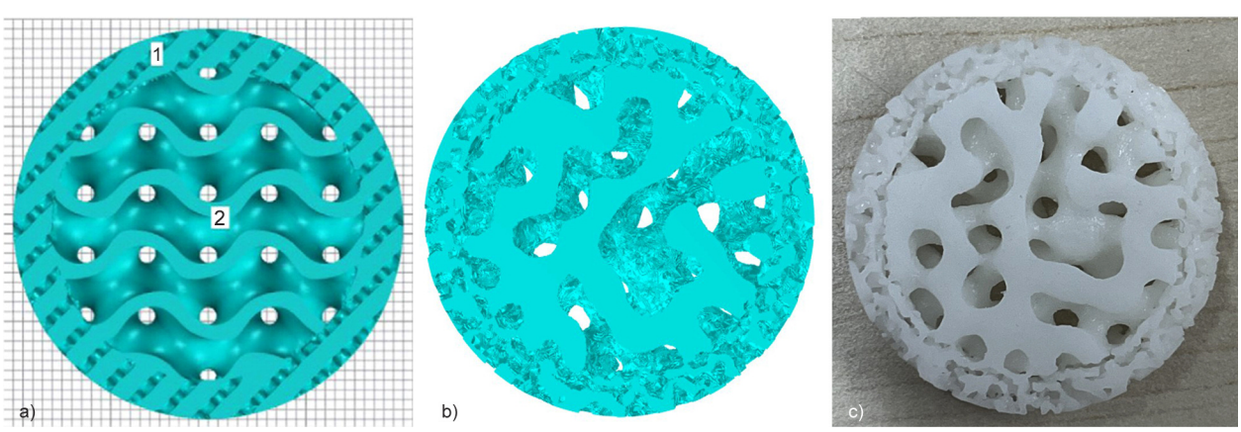


**Figure 3.** Femoral structure: a) femoral structure; b) femoral structure constructed by phase field method; c) 3D print of femoral structure.

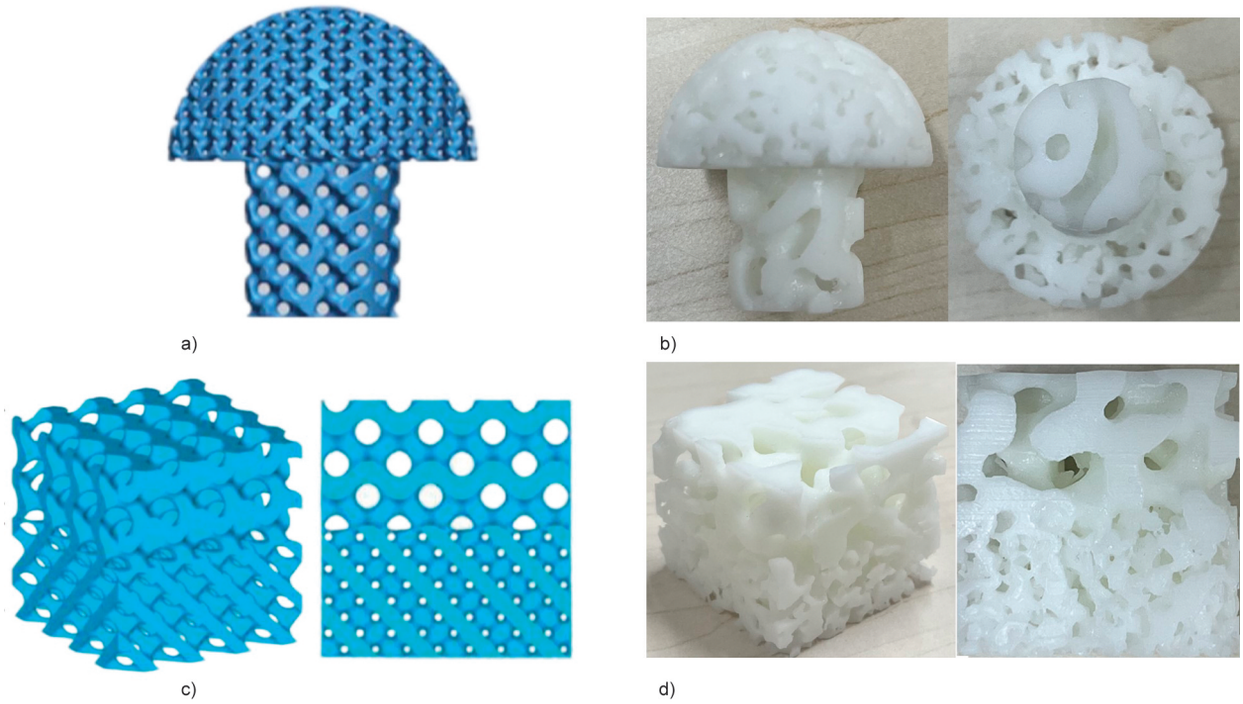


**Figure 4.** Gradient porous structures: a) hybrid cylinder/half-sphere shaped scaffold; b) hybrid cylinder/half-sphere shaped scaffold constructed by phase field method; c) gradient cube structure; d) gradient cube structure constructed by phase field method.

equivalent pore size of the hemisphere part is 0.59 mm.

While Figure 4c displays a gradient cube structure with a side length of 36 mm. Employing the phase field method outlined in this paper, the maximum cell size is 1.33 mm, the minimum cell size is 0.144 mm, and the number of grid cells is 334 988. The interfacial tension σ (in N/m) is a piecewise function relative to the temperature $T$ (in K). The temperature gradient is along the Z axis, when $0 \leq T \leq 18$, $\sigma = 3$, when $18 < T \leq 36$, $\sigma = 750$. The interface thickness $\varepsilon_{pf}$ is $1 \cdot 10^{-3}$ m, and the mobility $\chi$ is 1 m·s/kg. The 3D printed counterpart is produced using the SLA technique, as depicted in Figure 4d. The equivalent pore size of the upper part is 1.23 mm, and the equivalent pore size of the lower part is 0.54 mm.

The phase field method introduced in this paper, which designs gradient porous structures through the application of temperature fields, demonstrates practical viability, enabling rapid and precise control over pore size distribution. The resulting gradient porous structures are characterized by their irregular pores, seamless transition zones across varying pores, and interconnected pore networks. This contributes to the enhanced optimization of their multifunctional properties.

## 5. Conclusions

This paper establishes a flow-phase field dynamics model rooted in the phase separation behavior of two-phase immiscible co-continuous polymer blends, laying the groundwork for a novel geometric modeling approach for gradient porous structures guided by phase field theory. This approach addresses the shortcomings of conventional modeling techniques, such as high energy demands, uniform pore structures, and limited variability in pore size distribution. Through meticulous manipulation of phase field parameters and strategic design of the temperature field, it facilitates the efficient geometric modeling of gradient porous structures with varied pore size distributions. This method is suited for additive manufacturing, promising broad application across diverse sectors including machinery, energy, medical, construction, and aerospace, enhancing properties such as mechanical strength, sound absorption, and heat transfer. This innovative approach significantly cuts costs, fuels the development of advanced porous materials, and streamlines the research and development process.

Future research based on the methodologies introduced in this study will delve into the intricate relationships between phase field control parameters and

porosity. This is to devise more comprehensive strategies for constructing increasingly complex gradient porous structures.

## Acknowledgements

The present work was financially supported by the National Key R&D Program of China (No.2022YFC2009504).

## References

[1] Gupta K., Meena K.: Artificial bone scaffolds and bone joints by additive manufacturing: A review. Bioprinting, **31**, e00268 (2023). https://doi.org/10.1016/j.bprint.2023.e00268

[2] Distefano F., Pasta S., Epasto G.: Titanium lattice structures produced *via* additive manufacturing for a bone scaffold: A review. Journal of Functional Biomaterials, **14**, 125 (2023). https://doi.org/10.3390/jfb14030125

[3] Chen H., Han Q., Wang C., Liu Y., Chen B., Wang J.: Porous scaffold design for additive manufacturing in orthopedics: A review. Frontiers in Bioengineering and Biotechnology, **8**, 609 (2020). https://doi.org/10.3389/fbioe.2020.00609

[4] Zhao H., Han Y., Pan C., Yang D., Wang H., Wang T., Zeng X., Su P.: Design and mechanical properties verification of gradient voronoi scaffold for bone tissue engineering. Micromachines, **12**, 664 (2021). https://doi.org/10.3390/mi12060664

[5] Lv Y., Wang B., Liu G., Tang Y., Lu E., Xie K., Lan C., Liu J., Qin Z., Wang L.: Metal material, properties and design methods of porous biomedical scaffolds for additive manufacturing: A review. Frontiers in Bioengineering and Biotechnology, **9**, 641130 (2021). https://doi.org/10.3389/fbioe.2021.641130

[6] Maggay I. V., Chang Y., Venault A., Dizon G. V., Wu C-J.: Functionalized porous filtration media for gravity-driven filtration: Reviewing a new emerging approach for oil and water emulsions separation. Separation and Purification Technology, **259**, 117983 (2021). https://doi.org/10.1016/j.seppur.2020.117983

[7] Cao J., Wang W., Feng S.: A hierarchically porous sponge for stabilized emulsion separation with high filtration flux and separation efficiency. Journal of Materials Chemistry A, **10**, 10540–10547 (2022). https://doi.org/10.1039/d2ta01897g

[8] Zhang B., Wang W., Liang L., Xu Z., Li X., Qiao S.: Prevailing conjugated porous polymers for electrochemical energy storage and conversion: Lithium-ion batteries, supercapacitors and water-splitting. Coordination Chemistry Reviews, **436**, 213782 (2021). https://doi.org/10.1016/j.ccr.2021.213782

[9] Chuhadiya S., Himanshu , Suthar D., Patel S., Dhaka M.: Metal organic frameworks as hybrid porous materials for energy storage and conversion devices: A review. Coordination Chemistry Reviews, **446**, 214115 (2021). https://doi.org/10.1016/j.ccr.2021.214115

[10] Alhusseny A., Al-Aabidy Q., Al-Zurfi N., Nasser A., Aljanabi M.: Cooling of high-performance electronic equipment using graphite foam heat sinks. Applied Thermal Engineering, **191**, 116844 (2021). https://doi.org/10.1016/j.applthermaleng.2021.116844

[11] Tao Y., Ren M., Zhang H., Peijs T.: Recent progress in acoustic materials and noise control strategies – A review. Applied Materials Today, **24**, 101141 (2021). https://doi.org/10.1016/j.apmt.2021.101141

[12] Liu B., Cao W., Zhang L., Jiang K., Lu P.: A design method of voronoi porous structures with graded relative elasticity distribution for functionally gradient porous materials. International Journal of Mechanics and Materials in Design, **17**, 863–883 (2021). https://doi.org/10.1007/s10999-021-09558-6

[13] Feng J. W., Fu J. Z., Yao X. H., He Y.: Triply periodic minimal surface (TPMS) porous structures: From multi-scale design, precise additive manufacturing to multi-disciplinary applications. International Journal of Extreme Manufacturing, **4**, 022001 (2022). https://doi.org/10.1088/2631-7990/ac5be6

[14] Ma S., Tang Q., Zhu C., Wang F., Feng Q., Song J., Setchi R., Ma C., Tao R.: Laser powder bed fusion-built Ti6Al4V bone scaffolds composed of sheet and strut-based porous structures: Morphology, mechanical properties, and biocompatibility. Chinese Journal of Mechanical Engineering: Additive Manufacturing Frontiers, **1**, 100051 (2022). https://doi.org/10.1016/j.cjmeam.2022.100051

[15] Yao D., Zhang W., Zhou J. G.: Controllable growth of gradient porous structures. Biomacromolecules, **10**, 1282–1286 (2009). https://doi.org/10.1021/bm900008d

[16] Shen H., Yao D., Zhang W., Ye Q.: Modeling and simulation of the process for the generation of gradient porous structures from immiscible polymer blends. Journal of Manufacturing Science and Engineering, **142**, 031001 (2020). https://doi.org/10.1115/1.4045722

[17] Tourret D., Liu H., Llorca J.: Phase-field modeling of microstructure evolution: Recent applications, perspectives and challenges. Progress in Materials Science, **123**, 100810 (2022). https://doi.org/10.1016/j.pmatsci.2021.100810

[18] Yue P., Zhou C., Feng J. J., Ollivier-Gooch C. F., Hu H. H.: Phase-field simulations of interfacial dynamics in viscoelastic fluids using finite elements with adaptive meshing. Journal of Computational Physics, **219**, 47–67 (2006). https://doi.org/10.1016/j.jcp.2006.03.016

[19] Hamdia K. M., Ghasemi H.: Quantifying the uncertainties in modeling soft composites *via* a multiscale approach. International Journal of Solids and Structures, **256**, 111959 (2022). https://doi.org/10.1016/j.ijsolstr.2022.111959

[20] Yang N., Zhou K.: Effective method for multi-scale gradient porous scaffold design and fabrication. Materials Science and Engineering C, **43**, 502–505 (2014). https://doi.org/10.1016/j.msec.2014.07.052

[21] Yoo D-J., Kim K-H.: An advanced multi-morphology porous scaffold design method using volumetric distance field and beta growth function. International Journal of Precision Engineering and Manufacturing, **16**, 2021–2032 (2015). https://doi.org/10.1007/s12541-015-0263-2

[22] Maskery I., Aremu A. O., Parry L., Wildman R. D., Tuck C. J., Ashcroft I. A.: Effective design and simulation of surface-based lattice structures featuring volume fraction and cell type grading. Materials and Design, **155**, 220–232 (2018). https://doi.org/10.1016/j.matdes.2018.05.058